European Journal of Orthodontics, 2017, 1–7
doi:10.1093/ejo/cjx001

Original article

Structural, morphological, compositional, and mechanical changes of palatal implants after use: a retrieval analysis

Marc Schätzle[1,*], Spiros Zinelis[2,*], Goran Markic[1], George Eliades[2] and Theodore Eliades[1]

[1]Clinic of Orthodontics and Paediatric Dentistry, Center of Dental Medicine, University of Zurich, Zurich, Switzerland, and [2]Department of Dental Biomaterials, School of Dentistry, National and Kapodistrian, University of Athens, Athens, Greece

*The first two authors have contributed equally to this study.

Correspondence to: Theodore Eliades, Clinic of Orthodontics and Paediatric Dentistry, Center of Dental Medicine, University of Zurich, Plattenstrasse 11, Zurich 8032, Switzerland. E-mail: theodore.eliades@zzm.uzh.ch

Summary

Purpose: The aim of this study was to characterize the surface, elemental, and mechanical alterations of orthodontic palatal implants after intraoral aging.

Materials and method: Nineteen consecutively retrieved implants (RET) after orthodontic treatment and three unused implants used as control (CON) were included in this study. Both groups were characterized non-destructively by Stereomicroscopy, Optical Profilometry (Sa, Sq, Sz, Sc), and SEM/EDX analysis and then destructively after metallogaphic preparation employing instrumented indentation testing (HM, E_{IT}, η_{IT}, and HV) and SEM/EDX at bone-implant interface.

Results: All retrieved implants showed a loss of gloss with the formation of bone-like formation on the majority of them. However, no differences in surface roughness parameters were identified between macroscopically intact and retrieved regions of implants. The elements precipitated on the surface were O, C, Ca, and P while traces of Na, K, Al, S, Cl, and Mg were also identified. The surface of control sample is characterized by small pits while only Ti and Al traces were identified by EDX analysis. The presence of all the aforementioned elements apart from Ti and Al on the retrieved implants' surface should be appended to the contact of implant with bone and biological fluids while Interfacial analysis revealed a well-formed bone-implant interface. However, no significant differences were found for all mechanical properties tested between RET and CON groups.

Conclusions: The results of this study indicate that retrieved palatal implant surface has undergone morphological and elemental alterations probably associated with the osseointegration process during service. Insertion and functional loading did not affect the mechanical properties of implants tested.

Introduction

In orthodontic treatment, reliable anchorage is required in various treatment approaches to achieve a satisfactory result. Traditionally, the most common appliance for anchorage was a headgear which is predominantly dependent on patient cooperation ((1, 2)). More than 2 decades ago, temporary anchorage devices (TAD) were introduced ((3–7)). TADs offer reliable and predictable skeletal anchorage for orthodontic treatment, independent of patient cooperation, and are well-accepted by patients (2, 8, 9). Comparing different TADs, it has been shown that rough-surfaced palatal implants and miniplates have a statistical significantly higher survival rate than miniscrews (10).

The simplicity in use of palatal implants, minimal stress experienced during surgical implant installation and removal, as well as the reliable success rates of palatal implants are prerequisites for the high acceptance of this treatment by orthodontic patients (10–14).

Currently, there is little evidence on the profile of palatal implants surface during service, including structural alterations, changes in the mechanical properties, and various tissue-material interactions. Used titanium-alloy miniscrew implants show morphologic and surface structural alterations including adsorption of an integument that was calcified as a result of contact of the implants with biologic fluids and adjacent bone. Randomly organized osseointegration islets on these smooth titanium-alloy miniscrew surfaces might be enhanced by the extended period of retention in alveolar bone in spite of the smooth surface and immediate loading pattern of these implants (15).

The purpose of this study was to assess possible alterations in morphologic, compositional, and mechanical properties of rough-surfaced palatal implants after intraoral aging. The hypothesis was that retrieved palatal implants have surface, and mechanical property alterations after use.

Materials and methods

Sample collection

Twenty two palatal implants of the same manufacturer (Orthosystem® Palatal Implant, Institut Straumann AG, Basel, Switzerland) were included in this study. Eighteen implants were retrieved after successful orthodontic treatment while one was retrieved due to increased mobility (implant failure). All retrieved implants (RET) are appeared in Figure 1 classified on *in vivo* aging time. The median intraoral time was 43 months with 31.5 and 63 months indicating the 25th and 75th percentiles, respectively. The minimum intraoral time was 18 months and 96 months the maximum. Three unused implants were used as control (CON; Figure 2). Both groups were investigated initially by non-destructive and then by destructive experimental methods.

Optical microscopy (Stereomicroscopy)

The surface of all implants were studied under a stereomicroscope (Leica M80, Leica Microsystems, Wetzlar, Germany) and photographed with a digital camera (Leica DFC295, Leica Microsystems), which was coupled to the microscope.

Optical profilometry

Three root regions from the three unused implant and three retrieved implants free of macroscopically identified integuments were evaluated by an optical interferometric profiler (Wyko NT1100,Veeco, Tuscon, AZ, USA) operated under the following conditions: vertical scanning mode, Mirau lens (20 × 2), 40 µm vertical scan length, 113 × 148.5 µm acquisition window (×41.6 magnification), cylinder/tilt corrections, 25 l/mm high-pass Gaussian Fourier filtering (to remove surface waviness interferences), and 0.1 nm (z-axis), and 0.2 µm (x- and y-axes) resolution. Three amplitude parameters Sa (arithmetic mean deviation), Sz (the maximum height of the surface), and Sq (root mean square roughness), and one volume functional parameter Sc (core void volume) showing the volume the surface would support from 10 to 80 per cent of the bearing ratio were determined. All samples were analyzed with the same root–neck orientation.

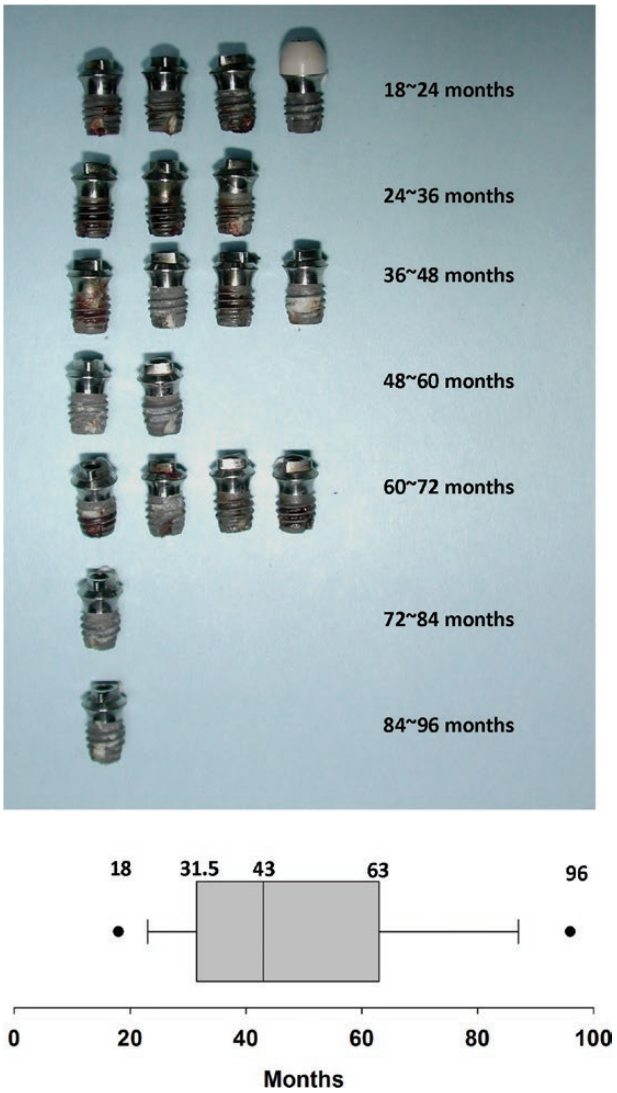

Figure 1. Photograph showing the retrieved implants classified in groups based on intraoral aging time. The side with the maximum integument coverage has been shown from the implant's surface. It is clear that the presence of white integuments increases over the aging time. The horizontal box plot indicates the median the 25th and 75th percentiles and the minimum and maximum intraoral time of the sample collected.

SEM/EDX analysis

Three as received and three retrieved implants were investigated by SEM/EDX analysis. Secondary electron (SE) and backscattered electron (BE) images were collected with a Scanning Electron Microscope (Quanta 200, FEI, Hillsboro, Ore) at high vacuum chamber conditions ($5.2 * 10^{-6}$ Torr pressure), 25 KV acceleration voltage, and 99 µA beam current. Furthermore, one X-ray energy dispersive (EDX) spectrum was recorded from each implant employing an X Flash 6|10 Silicon Drift Detector (Bruker, Berlin, Germany) under the aforementioned conditions and ×400 nominal magnification. The elemental distribution of probed elements for the retrieved samples was determined by EDX analysis employing an area scan mode at the same magnification.

Mechanical properties (instrumented indentation testing)

Three specimens from the retrieved group and the three unused implants were embedded in epoxy resin (Epofix, Struers, Belarup,

Denmark) along their longitudinal axis and cut in the middle with a diamond cut off wheel (Struers). The samples were ground from 220 to 2000 grit SiC papers and polished with diamond pastes (DP, Struers) up to 1 μm in a grinding polishing machine (Dap-V, Struers). Afterwards the surfaces were cleaned in an ultrasonic bath and Martens hardness (HM), indentation modulus (E_{IT}), elastic index (η_{IT}; the elastic to total work ratio), and the Vickers hardness (HV) were determined employing instrumented indentation testing (IIT) with a universal hardness-testing machine ZHU0.2/Z2.5 (Zwick Roell, Ulm, Germany). Five force indentation depth curves were recorded from each sample employing a Vickers indenter, 9.8 N load and 10 seconds contact time and the average values of HM, E_{IT}, η_{IT}, and HV were used to characterize the properties of each specimen.

Interfacial SEM/EDX analysis

After IIT, the retrieved specimens were sputter coated with carbon in a sputter-coating unit (SCD 004 Sputter-Coater) with OCD 30 attachment, Bal-Tec, Vaduz, Liechtenstein). One EDX spectrum were recorded from the cross-section on dental implant of both groups tested at ×300 magnification while SE and BE images were recorded at the implant-bone interface employing the aforementioned operating conditions and ×3000 nominal magnification. The gradients of Ti, O, Ca, and P at the interface were studied by line scan analysis employing 150 points of spot analysis for a total length of 42 μm.

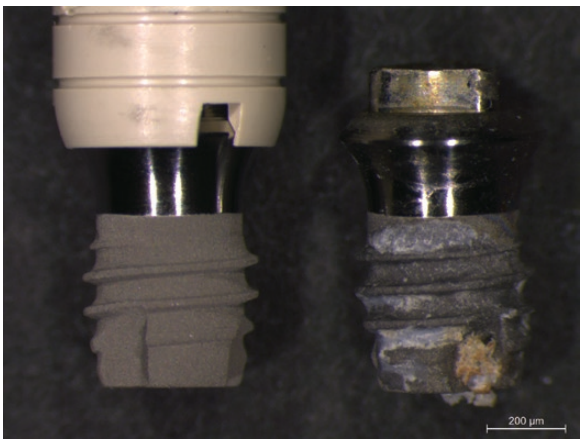

Figure 2. Representative optical images from the surface of CON (left) and RET groups (right). The retrieved implants have less gloss compared to control, while white and yellow bone-like formations are easily identified on their surface. CON, control implants; RET, retrieved implants.

Statistical analysis

All surface roughness parameters and mechanical properties values were statistically compared between CON and RET groups by unpaired *t*-test at 95 per cent level of significance ($a = 0.05$) after the normality of data was checked with Shapiro–Wilk and equal variance tests.

Results

Optical microscopy (Stereomicroscopy)

Figure 2 presents the surface of reference and representative retrieved implants. As it clearly shows also in Figures 1 and 2, the retrieved implants have lost their initial surface gloss while firmly attached white and yellow integuments are easily identified.

Optical profilometry

Representative 3D profilometric images are presented in Figure 3 while the roughness parameters are shown in Table 1. No statistical significant differences were identified for all parameters tested.

SEM/EDX analysis

Figure 4 demonstrates low magnification SE images from CON and RET groups where the attached integuments are identified as darker areas in BE due to lower mean atomic number compared to Ti. Higher magnification images (Figure 5) show that the reference surface is characterized by shallow grooves and micro pits, while the surface of retrieved implants illustrates intact regions along with regions covered by intraoral integuments. The latter are easily distinguished due to their darker appearance in BE image (lower mean atomic number contrast; Figure 5). EDX analysis revealed that reference implant surfaces consists mainly of Ti and traces of O and Al, while the surface

Table 1. Mean values and standard deviations in parentheses of roughness parameters tested. No statistical significant differences for all parameters were identified after statistical analysis ($P > 0.05$). CON, control implants; RET, retrieved implants.

Groups	Sa (μm)	Sz (μm)	Sq (μm)	Sc (μm³/μm²)
CON	3.6 (0.6)	25.3 (3.3)	4.4 (0.7)	5.5 (1.2)
RET	2.5 (0.8)	22.6 (4.2)	3.2 (0.9)	3.5 (1.3)

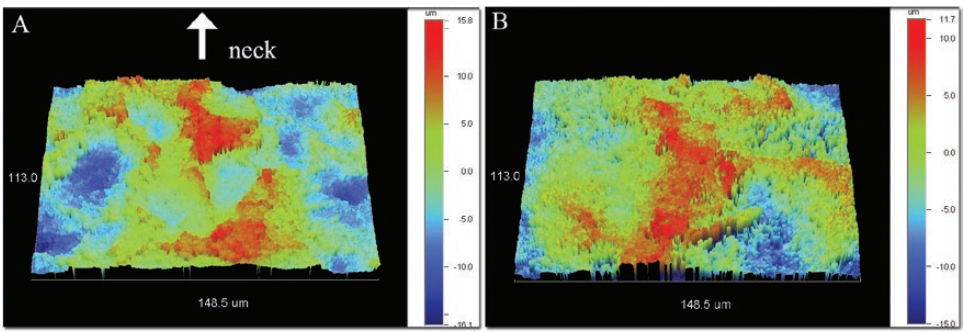

Figure 3. Representative 3D optical profilometric images from CON (A) and RET (B) implant surfaces. Both images have the same root–neck orientation indicated by the white arrow.CON, control implants; RET, retrieved implants.

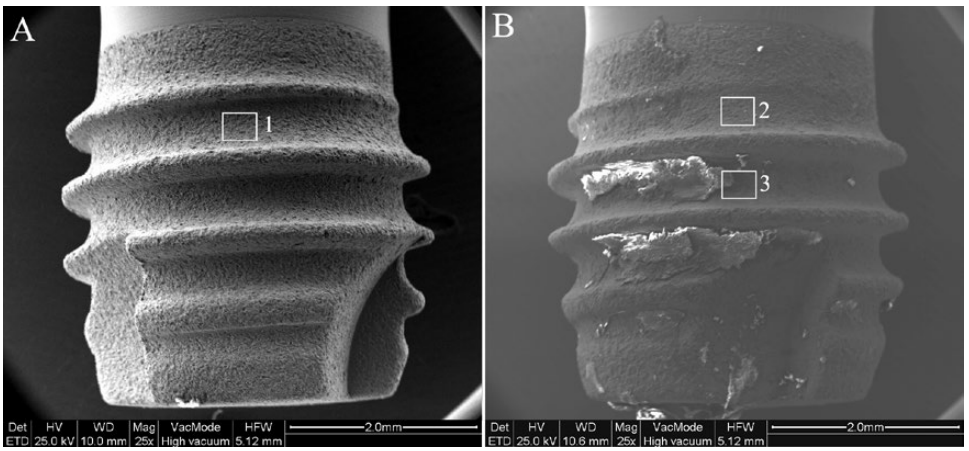

Figure 4. SE images from the surface of CON (A) and RET (B) groups. The presence of bone-like integuments is easily identified within serrations. The regions 1 and 2 outlined by white rectangular indicate the locations where the higher magnification BE images were acquired. The region 3 presents the area of X-ray mapping where a part of bone-like formation was also included. (Original magnification: ×25, bar 2 mm). BE, backscattered electron; CON, control implants; RET, retrieved implants; SE, secondary electron.

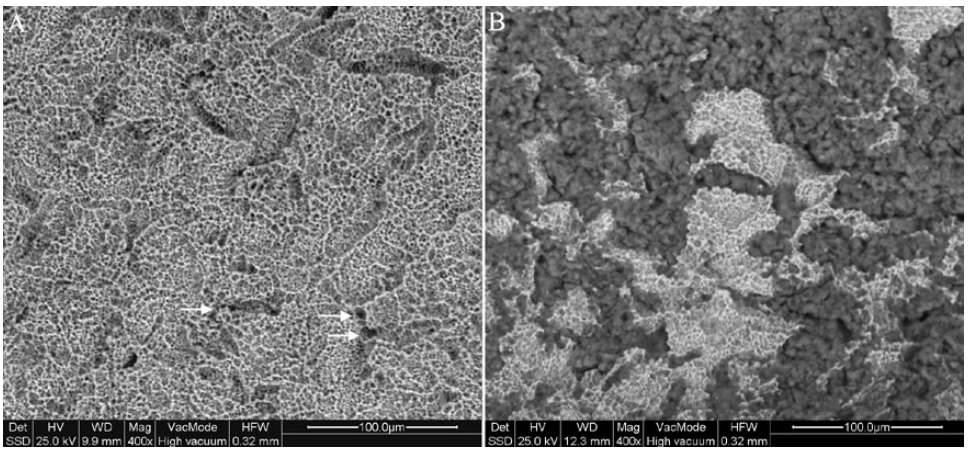

Figure 5. (A) Representative BE image from the surface of control group with shallow grooves and pits and a random distribution of tiny regions of low atomic contrast in the valleys (a few pointed by the white arrows). (B) BE from the surface of retrieved implants where the metallic substrate is covered by a randomly distributed lower mean atomic number phase (original magnification ×400, bar 100 µm). BE, backscattered electron.

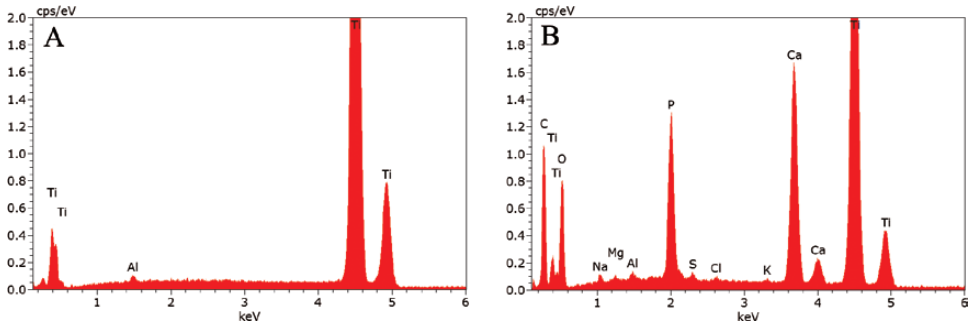

Figure 6. Representative EDX spectra from the surface of CON (A) and RET (B) implants. CON, control implants; EDX, x-ray energy dispersive; RET, retrieved implants.

of retrieved implants has been enriched mainly by C, O, Ca, and P and traces of Na, Mg, K, S, and Cl (Figure 6). BE image and X-ray distribution of C, N, O, P, Ca, Ti, Al, Mg, Na S, and Si are presented in Figure 7. C, N, and Ti illustrate random distributions. P and Ca depict similar distribution and in extent complementary to C distribution. All the rest elements present similar distributions.

Mechanical properties

Two representative force indentation depth curves from both groups are appeared in Figure 8. The results of mechanical properties tested are presented in Table 2 with no significant difference between the two groups.

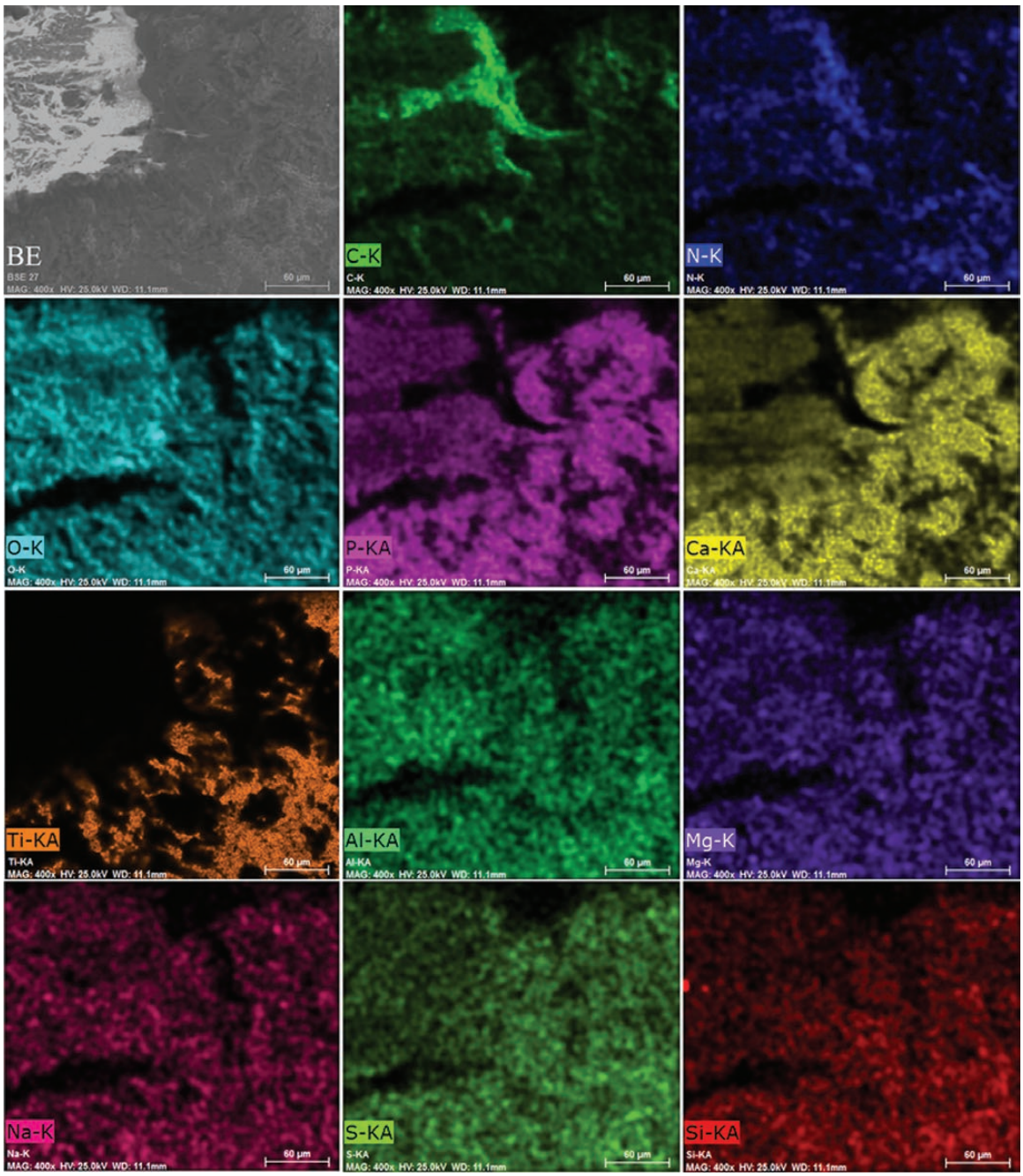

Figure 7. BE image and X-ray distribution of C, N, O, P, Ca, Ti, Al, Mg, Na, S, and Si. C, N, and Ti illustrate a random distribution, while similar distribution depict O, Al, Mg, Na, S, and Si. P and Ca illustrate also similar distribution and in extent complementary to C distribution (bar 60 μm). BE, backscattered electron.

SEM/EDX interfacial analysis

An EDX spectrum from the cross-section of implant is presented in Figure 9 where only Ti was identified. High magnification interfacial analysis revealed a well formed and defined interface between implant and bone (Figure 10). Line scan analysis (Figure 11) demonstrates that Ti has a progressively reduction from metal to bone while O, Ca, and P showed the inverse behaviour. Interestingly, O has reached the maximum value at implant-bone interface while Ca and P further in bone structure.

Table 2. Mean values and standard deviations in parentheses of mechanical properties tested. No statistical significant differences were identified between two groups ($P > 0.05$). CON, control implants; E_{IT}, indentation modulus; HM, Martens hardness; HV, Vickers hardness; η_{IT}, elastic index; RET, retrieved implants.

Groups	HM (N/mm²)	E_{IT} (GPa)	η_{IT} (%)	HV
CON	2097 (83)	56 (3)	29 (1)	274 (5)
RET	2176 (71)	55 (4)	28 (1)	282 (6)

Discussion

Based on the results of this study the null hypothesis should be partially accepted as retrieved implants demonstrate only surface and morphological alterations after *in vivo* aging. The analysis of retrieved implants has gained increased interest in the last years as a tool to elucidate the failure mechanism of dental implants after *in vivo* aging. The development of international standards (16, 17) for handling and testing retrieved implants is indicative for the significance of this methodology to characterize the underlying failure mechanisms. In an effort to eliminate further variability due to the placement of palatal implants in several patients only a palatal implant from a single manufacturer was included in this study.

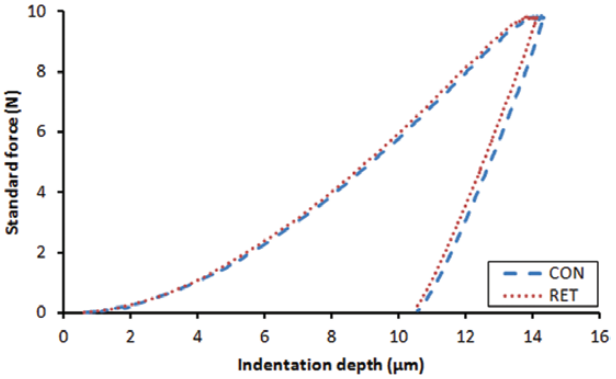

Figure 8. Representative load indentation depth curves for both groups tested.

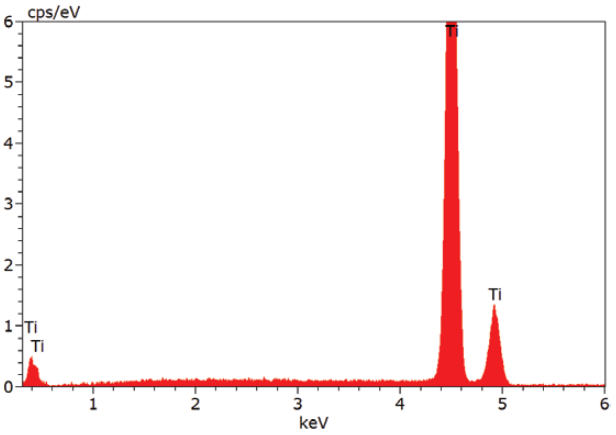

Figure 9. EDX spectrum from the cross-section of implants tested. EDX, X-ray energy dispersive.

The experimental part of this study provides a substantial piece of information for the surface and bulk properties of tested implants before intraoral placements. Both 3D profilometric and the higher magnification SE images show that the surface structure comprises of shallow grooves and small pits, typical features of SLA procedure. The former is appended to grit sandblasting of implant surface and the latter to the following acid etching (18). The Sa value of tested implant 3.6 ± 0.6 μm was found within to previously reported range of Sa (2.5 to 3.0 μm) values for dental implants (19) while according to Alberktsson's classification the surface of palatal implant is categorized as moderately rough (20). Ti is the only element identified after EDX analysis of the cross–section, while traces of Al were also identified on the implant surface denoting that the implant is made of commercially pure Ti. The presence of Al on the treated implant surface should be appended to the retention of alumina fragments after surface roughening process. Although HM is increasingly used in materials science characterization (21) as a more reliable hardness-testing free of various complications associated with Vickers procedure (22), HV was also determined for comparison with literature data. Interestingly, the HV (Table 2) was found higher than the nominal value of cp Ti (180 HV) implying a previous thermomechanical process. Furthermore, the E_{IT} was less than half the nominal Young modulus of Ti (103GPa) a finding attributed to the fact that E_{IT} cannot be reliable measured in non-stress free samples as it happens with heavily cold worked alloys where a residual stress field has been developed after thermomechanical treatment.

As it was expected all retrieved implants demonstrated a loss of gloss due to the adsorption of biological fluids, and the development of retained oral integuments and bone-like formations (Figures 2B, 4B, and 5B). Although in this study the bone-like formations did not quantify (i.e. bone-implant contact measurement) it is profound from Figure 1 that these formations are more likely to be observed on implants with increased intraoral time (Figure 1). Despite the intraoral aging BE image of retrieved samples (Figure 5B) demonstrate that part of the surface remained free of intraoral integuments

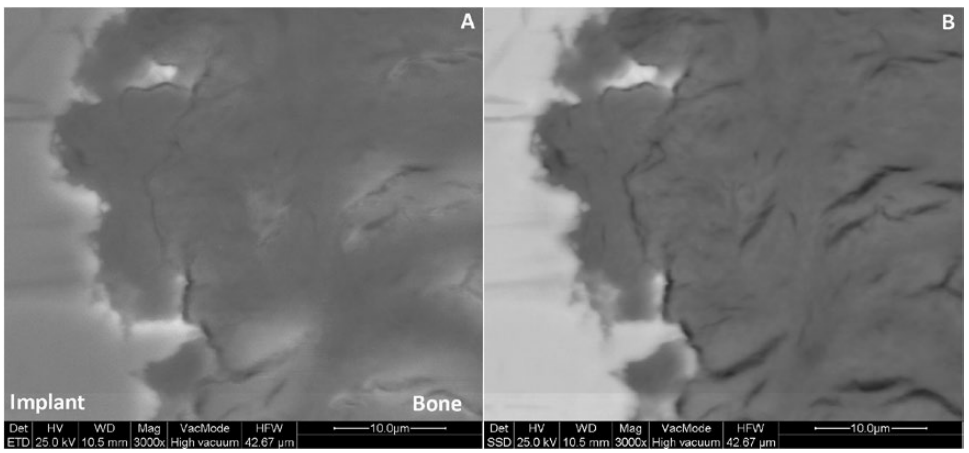

Figure 10. Representative SE (A) and BE (B) images from the implant-bone interface of retrieved palatal implants. BE, backscattered electron; SE, secondary electron.

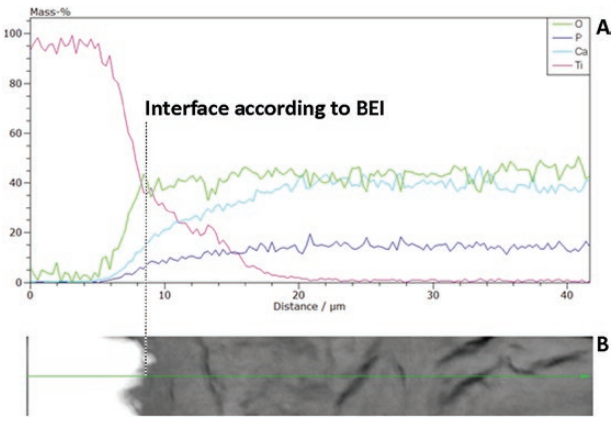

Figure 11. Line scan EDX analysis for Ti, O, P, and Ca of the implant-bone interface (A). The bottom shows part of the BE image of figure where the line scan was recorded (B). BE, backscattered electron; EDX, x-ray energy dispersive.

and thus might explain why the roughness parameters of macroscopically intact retrieved implants remain unaffected by intraoral aging (Table 1). The elemental composition of retrieved surface with bone-like formation are dominated by the presence of Ca and F (Figures 6 and 7) and less amounts of C, O, Na, Mg, Al, S, Cl, and K, all of them of biological origin. The presence of these elements has been also identified in retrieved orthodontic miniscrew implants (15) and generally it is considered as a typical aging profile for implantable metallic materials (23) involving in first place the adsorption of proteinaceous integuments with subsequent calcification in second place with the precipitation of F and Ca. The cross-section analysis (Figures 9 and 10) revealed a distinct and well-formed interface denoting a rather well adhesion of bone-like integuments to implant surface. This might not be desirable for orthodontic palatal implants from a clinical standpoint as their placements is considered temporarily and the removal of bone may trauma the bone increasing patient discomfort and healing time. No differences in mechanical properties tested were determined implying that neither insertion nor functional loading exerted enough high stresses to trigger a degradation mechanism.

The results of this retrieval analysis suggest that the placement and subsequent long-term orthodontic loading of rough-surfaced palatal implants would not affect their mechanical properties. Furthermore, retrieved palatal implant surface has undergone morphological and elemental alterations. The absorbed formations could have been the result of calcification of absorbed integument probably associated with the osseointegration process, which might complicate the non-invasive removal of implants. Insertion, functional loading, and subsequent explantation did not affect the mechanical properties of implants tested.

Conflict of Interest

None to declare.

References

1. Nanda, R.S. and Kierl, M.J. (1992) Prediction of cooperation in orthodontic treatment. *American Journal of Orthodontics and Dentofacial Orthopedics*, 102, 15–21.
2. Jambi, S., Thiruvenkatachari, B., O'Brien, K.D. and Walsh, T. (2013) Orthodontic treatment for distalising upper first molars in children and adolescents. *Cochrane Database Systematic Review*, 23, CD008375.
3. Triaca, A. (1992) Titan-Flachschrauben-Implantat zur orthodontischen Verankerung am anterioren Gaumen. *Informationen der Orthodontie und Kieferorthop*, 24, 251–257.
4. Wehrbein, H., Glatzmaier, J., Mundwiller, U. and Diedrich, P. (1996) The Orthosystem–a new implant system for orthodontic anchorage in the palate. *Journal of Orofacial Orthopedics*, 57, 142–153.
5. Glatzmaier, J., Wehrbein, H. and Diedrich, P. (1995) [The development of a resorbable implant system for orthodontic anchorage. The BIOS implant system. Bioresorbable implant anchor for orthodontic systems]. *Fortschr Kieferorthop*, 56, 175–181.
6. Kanomi, R. (1997) Mini-implant for orthodontic anchorage. *Journal of Clinical Orthodontics: JCO*, 31, 763–767.
7. Costa, A., Raffainl, M. and Melsen, B. (1998) Miniscrews as orthodontic anchorage: a preliminary report. *The International Journal of Adult Orthodontics and Orthognathic Surgery*, 13, 201–209.
8. Gündüz, E., Schneider-Del Savio, T.T., Kucher, G., Schneider, B. and Bantleon, H.P. (2004) Acceptance rate of palatal implants: a questionnaire study. *American Journal of Orthodontics and Dentofacial Orthopedics*, 126, 623–626.
9. Feldmann, I., List, T., Feldmann, H. and Bondemark, L. (2007) Pain intensity and discomfort following surgical placement of orthodontic anchoring units and premolar extraction: a randomized controlled trial. *The Angle Orthodontist*, 77, 578–585.
10. Schätzle, M., Männchen, R., Zwahlen, M. and Lang N.P. (2009) Survival and failure rates of orthodontic temporary anchorage devices: a systematic review. *Clinical Oral Implants Research*, 20, 1351–1359.
11. Jung, B.A., *et al.* (2007) Early loading of plalatal implants (ortho-type II) a prospective multicenter randomized controlled clinical trial. *Trials*, 8, 24.
12. Jung, B.A., Kunkel, M., Göllner, P., Liechti, T. and Wehrbein, H. (2009) Success rate of second-generation palatal implants. *The Angle Orthodontist*, 79, 85–90.
13. Jung, B.A., Kunkel, M., Göllner, P., Liechti, T., Wagner, W. and Wehrbein, H. (2012) Prognostic parameters contributing to palatal implant failures: a long-term survival analysis of 239 patients. *Clinical Oral Implants Research*, 23, 746–750.
14. Karagkiolidou, A., Ludwig, B., Pazera, P., Gkantidis, N., Pandis, N. and Katsaros, C. (2013) Survival of palatal miniscrews used for orthodontic appliance anchorage: a retrospective cohort study. *American Journal of Orthodontics and Dentofacial Orthopedics*, 143, 767–772.
15. Eliades, T., Zinelis, S., Papadopoulos, M.A. and Eliades, G. (2009) Characterization of retrieved orthodontic miniscrew implants. *American Journal of Orthodontics and Dentofacial Orthopedics*, 135, 10.e1–10.e7; discussion 10.
16. ISO 12891-1 (2015) *Retrieval and Analysis of Surgical Implants -Part 1: Retrieval and Handling*. Geneva, Switzerland.
17. ISO 12891-2 (2014) Retrieval and analysis of surgical implants -Part 2: Analysis of retrieved surgical implants. Geneva, Switzerland.
18. Le Guéhennec, L., Soueidan, A., Layrolle, P. and Amouriq, Y. (2007) Surface treatments of titanium dental implants for rapid osseointegration. *Dental Materials*, 23, 844–854.
19. Eom, T.G., *et al.* (2012) Experimental study of bone response to hydroxyapatite coating implants: bone-implant contact and removal torque test. *Oral Surgery, Oral Medicine, Oral Pathology and Oral Radiology*, 114, 411–418.
20. Albrektsson, T. and Wennerberg, A. (2004) Oral implant surfaces: Part 1–review focusing on topographic and chemical properties of different surfaces and *in vivo* responses to them. *The International Journal of Prosthodontics*, 17, 536–543.
21. Zinelis, S., Al Jabbari, Y.S., Gaintantzopoulou, M., Eliades, G. and Eliades, T. (2015) Mechanical properties of orthodontic wires derived by instrumented indentation testing (IIT) according to ISO 14577. *Progress in Orthodontics*, 16, 19.
22. Shahdad, S.A., McCabe, J.F., Bull, S., Rusby, S. and Wassell, R.W. (2007) Hardness measured with traditional Vickers and Martens hardness methods. *Dental Materials*, 23, 1079–1085.
23. Eliades, T., Eliades, G., Athanasiou, A.E. and Bradley, T.G. (2000) Surface characterization of retrieved NiTi orthodontic archwires. *European Journal of Orthodontics*, 22, 317–326.